JOURNAL OF CATALYSIS 144, 495–505 (1993)

Hexane Cracking in ZSM-5: *In Situ* ^{13}C Cross-Polarization Magic-Angle-Spinning NMR and Flow Reactor/GC Experiments

A. K. NOWAK, A. E. WILSON, K. ROBERTS, AND K. P. DATEMA

Koninklijke/Shell-Laboratorium Amsterdam (Shell Research B.V.), Badhuisweg 3, 1031 CM Amsterdam, The Netherlands

Received June 26, 1992; revised June 11, 1993

The conversion of *n*-hexane by ZSM-5 has been studied in closed samples by ^{13}C cross-polarization (CP) magic-angle-spinning (MAS) NMR and by flow reactor/GC analysis. The NMR experiments, carried out after various heat treatments and subsequent quenching of the sealed samples to room temperature, result in product distributions which are comparable to those from flow reactor/GC experiments at full conversion, with propane (47 mol%) and butanes (25 mol%) as the main products. The differences in product distributions observed by NMR and the flow reactor/GC experiments, especially the absence of olefins in all NMR experiments, are ascribed to the difference in contact time in the two experimental setups. Based on the complementary data obtained from the two techniques, it is proposed that, at temperatures below 300°C, isomerization to the methylpentanes is dominant, while at higher temperatures cracking of the reactant and the methylpentanes takes over. Dimethylbutanes could not be detected by NMR, and it is concluded that the formation of these isomers is inhibited in the medium-pore zeolite.

INTRODUCTION

Despite the large-scale application of zeolite catalysts in cracking processes there is still considerable uncertainty as to the detailed mechanism of the reaction. Nevertheless, a general picture of the cracking mechanism has emerged, based on results from model hydrocracking (*1*, *2*) and cracking (*3–5*) reactions, which unites various mechanisms observed in other catalytic systems.

It has been proposed that two cracking mechanisms occur concurrently (*6*): one resembles the classical bimolecular carbenium-ion mechanism which has been demonstrated in liquid-acid systems (*7*), and the other a monomolecular one involving the direct protonation of the saturated hydrocarbons as observed in superacid systems (*8*). Radical processes have also been discussed as possibilities. To date, no conclusive proof for any of the proposed mechanisms has been brought forward, which is ascribed to the fact that reacting species inside the pores of zeolite crystallites are difficult to observe. However, product distributions varying with temperature (*4*), the structure of the catalyst (*4*), the partial pressure of the feed (*6*), and the conversion (*3*, *5*) can be explained by assuming varying contributions of the different mechanisms.

It is desirable, especially when reaction mechanisms are being studied, to be able to detect species during the reaction inside the catalyst particles. Most experiments, however, are based on chromatographic or spectroscopic analysis of the reaction products after they have left the reactor.

The potential of ^{13}C cross-polarization (CP) magic-angle-spinning (MAS) NMR for monitoring hydrocarbon conversions taking place inside the catalyst particles using sealed capsule samples ("*in situ* NMR") was demonstrated recently (*9*). In an *in situ* NMR study of the conversion of ethene in ZSM-5 (*10*) several branched olefins could be detected inside the catalyst, albeit only at temperatures below 0°C. That study pro-

0021-9517/93 $5.00

vided indirect evidence that olefins formed in the conversion of paraffins are indeed rapidly converted due to the higher temperature employed in these reactions. Similar conclusions were drawn by White *et al.* (*11*) from their *in situ* NMR investigation of the oligomerization of propene in ZSM-5. In both studies there were indications of the existence of alkoxide species. In another reaction, the conversion of methanol by SAPO-34, no olefins could be detected in the NMR analysis of the closed system, whereas flow reactor/GC experiments demonstrated their presence clearly (*12*).

In this paper we report on the investigation of the cracking of *n*-hexane by ZSM-5 using the *in situ* ^{13}C NMR technique and the direct comparison of the results with those from a flow reactor/GC system. Conclusions are drawn with respect to the reaction mechanism and the compatibility of the two techniques in the study of paraffin conversions.

METHODS

^{13}C Cross-Polarization Magic-Angle-Spinning NMR

All NMR experiments were carried out on an H–ZSM-5 catalyst with Si/Al = 13. The zeolite samples were placed in Pyrex capsules and heated to 400°C overnight under vacuum. *n*-Hexane-1-^{13}C (10 mol%) was then allowed to adsorb at a pressure of about 2 kPa, resulting in a pore filling of about 8 molecules/unit cell (*13*). After they were sealed, the sample tubes were placed in an oven at the chosen reaction temperature for a short period of time; all temperatures and exposure times are listed in Table 1. The samples were then quenched to room temperature and placed in the NMR probe.

Spectra were collected using a Bruker MSL 300 spectrometer (carbon frequency 75.46 MHz) and a double-bearing CP-MAS probe using cross-polarization (2–3 ms contact time) and high-power proton decoupling with a B_1-field strength corresponding to a 90° pulse of 4–5 μs. The sample spinning rate was 900–1500 Hz. Adamantane with the upfield methine peak at 29.23 ppm (*12*) was used as an external reference. All ^{13}C CP MAS NMR measurements were performed at room temperature.

TABLE 1

ZSM-5/*n*-Hexane Sample Treatment Conditions

Sample	Temperature (°C)	Exposure period (min)
A	20	—
B	155	2
C	200	5
D	220	3
E	300	5
F	400	5

In order to accurately determine their chemical shifts in the sorbed state the expected conversion products were separately adsorbed on ZSM-5 in independent reference experiments. The observed NMR shifts are listed in Table 2. Liquid-state and adsorbed-state values from the literature are given for comparison. It can be seen that chemical shift differences of up to 1.5 ppm, e.g., for *n*-hexane, arise. We ascribe these differences to interactions occurring in the adsorbed phase or to differences in the magnetic susceptibility inside the zeolite. The results of the reference measurements clearly indicate that separate NMR measurements are necessary for unambiguous peak assignments.

Flow Reactor/GC Experiments

All flow experiments were performed in a fixed-bed reactor, using typically 25–50 mg of catalyst at 450°C and a pressure of 40 kPa following the procedure described by Wielers *et al.* (*4*). Nitrogen was used as carrier gas with an N_2/*n*-hexane ratio of 4 : 1. Experiments in which the conversion was varied systematically between 20 and 80% were performed on an H–ZSM-5 catalyst with Si/Al = 29 which, at a comparable level of activity, gave the same product distribution as the catalyst used in the NMR experiments at a conversion level of 20%. The

TABLE 2

Chemical Shifts of a Number of Small Hydrocarbons Sorbed in ZSM-5

Species	Carbon position	Chemical shift (ppm)			Present in sample
		Liquid-state	Adsorbed on ZSM-5		
			Reference	Observed[c]	
Methane	C_1	−2.3	−7.5	−7.0[b]	None
Ethane	C_1	5.7	6.8	6.7–7.6	D, E, F
Propane	C_1	15.4	16.3	16.1–16.4	B, C, D
	C_2	15.9	16.3	16.7–16.9	E, F
n-Butane	C_1	13.1	13.8	13.8	C, D, E
	C_2	24.9	26.2	26.0	F
i-Butane	C_1	24.3	24.2	24.6	D, E, F
	C_2	25.0	24.2	—[d]	
n-Pentane	C_1	14.3	14.4	—[e]	None
	C_2	23.7	23.8	—[e]	
	C_3	35.2	35.2	—[e]	
n-Hexane (feed)	C_1	13.7 (13.9)[a]	14.2	14.2	A, B, C
	C_2	22.8 (23.1)[a]	24.1	24.1	D
	C_3	31.9 (32.2)[a]	33.4	33.4	
2-Methylpentane	C_1	22.4	22.9	22.4	C, D
	C_2	27.6	28.3	—[d]	
	C_3	41.6	41.9	—[d]	
	C_4	20.5	21.2	—[d]	
	C_5	14.0	14.4	—[d]	
3-Methylpentane	C_1	11.1	11.3	11.0–11.3	C, D, E
	C_2	29.1	30.2	29.1	
	C_3	36.5	36.8	35.1	
	C_4	18.4	18.9	18.6	

Note. For comparison liquid-state data taken from Ref. (*14*) are also given. The reference NMR spectra were recorded by adsorption of single compounds or mixtures. The last column indicates the occurrence of the species in samples A–F.

[a] Liquid-state NMR values measured by us as a check of the values in Ref. (*14*).

[b] Not observed with CP/MAS (contact time is 3 ms), only with high-power proton decoupling/MAS technique.

[c] Our values agree well with those reported in Ref. (*15*) for propane, butanes, *n*-pentane, and *n*-hexane, whereas for methane and ethane a discrepancy of about 3 ppm occurs. This is due to the fact that the present data were obtained in CP mode to observe adsorbed species only, whereas those in Ref. (*15*) are obtained as average from adsorbed and gas-phase species.

[d] Signal overlaps or intensity too low for detection due to the selective labelling.

[e] Not observed.

conversion was adjusted by varying the weight hourly space velocity. Product analysis was performed on-line.

RESULTS

^{13}C *Cross-Polarization Magic-Angle-Spinning NMR*

All ^{13}C CP MAS NMR spectra, recorded under the conditions listed in Table 1, are shown in Figs. 1a–1f. The assigned chemical shifts are listed in Table 2.

Figure 1a shows the spectrum of the unheated sample A. It consists of three peaks originating from the C_1, C_2, and C_3 atoms, respectively, of adsorbed *n*-hexane. The strong intensity of the C_1 signal is due to the selective ^{13}C enrichment in this position. After exposure to 155°C for 2 min (Fig. 1b),

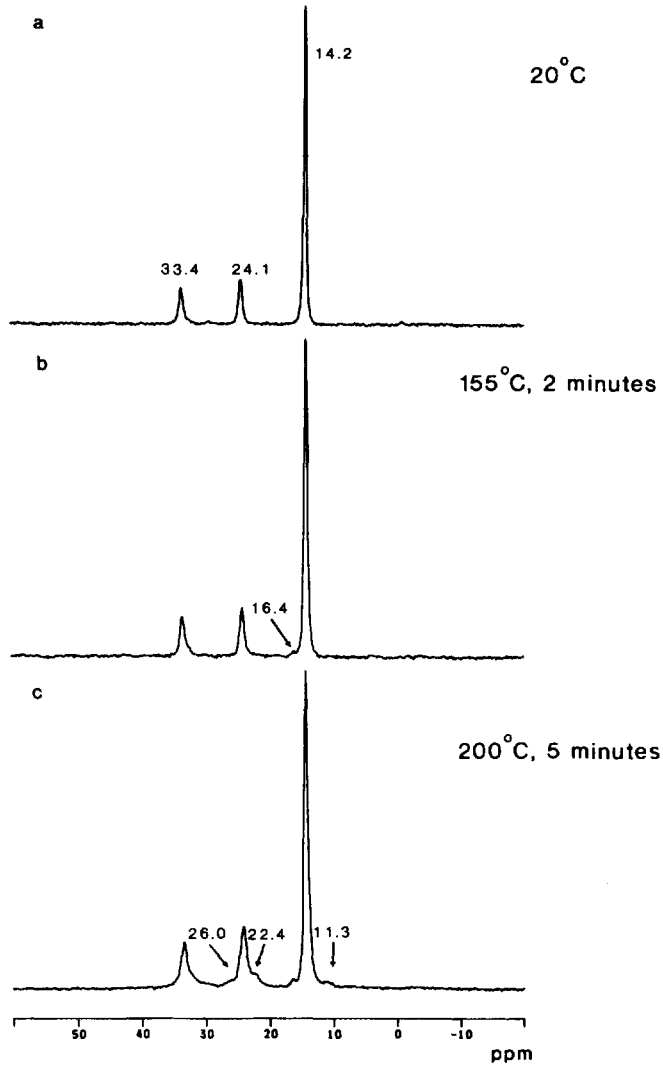

FIG. 1. 75.46 MHz ^{13}C CP MAS NMR spectra of ZSM-5 catalyst loaded with *n*-hexane (10 mol% carbon-13 enriched at the C_1 position in a sealed sample capsule after various reaction tempertures. The relaxation delay was 4–5 s at a contact time of 2–3 ms and a proton 90° pulse of 4–5 μs, the spectral width was at least 400 pm, and the sample spinning rate was 900–1500 Hz. The labelled chemical shifts are those which are new with respect to the previous spectrum. Note that the largest peak in the spectra shown in (a)–(d) stems from *n*-hexane, whereas that in (e) and (f) originates from propane. Exposure temperatures, number of scans, and chemical shift assignments of new signals, where applicable, with respect to previous spectra are given below. For the last spectrum (f) the complete chemical shift assignments are listed: (a) room temperature (1488 scans), *n*-hexane-C_1 (enriched) at 14.2 ppm, *n*-hexane-C_2 at 24.1 ppm, *n*-hexane-C_3 at 33.4 ppm; (b) 155°C (2084 scans), propane-C_1 at 16.4 ppm; (c) 200°C (16,400 scans), 3-methylpentane-C_1 at 11.3 ppm, 2-methylpentane-C_1 at 22.4 ppm, *n*-butane-C_2 at 26.0 ppm (*n*-butane-C_1 at 13.8 ppm overlaps with the *n*-hexane-C_1 signal at 14.2 and can only be observed separately in the absence of *n*-hexane in (e) and (f); (d) 220°C (6300 scans), ethane at 7.6 ppm, 3-methylpentane-C_4 at 18.6 ppm, *i*-butane-C_1 at 24.6 ppm, 3-methylpentane-C_2 at 29.1 ppm, 3-methylpentane-C_3 at 35.1 ppm; (e) 300°C (14,600 scans), propane-C_2 at 16.9 ppm; and (f) 400°C (12,770 scans), ethane at 6.7 ppm, propane at 16.1 ppm and shoulder at 16.9 ppm, *n*-butane at 13.8 ppm and 26.0 ppm, and *i*-butane at 24.6 ppm.

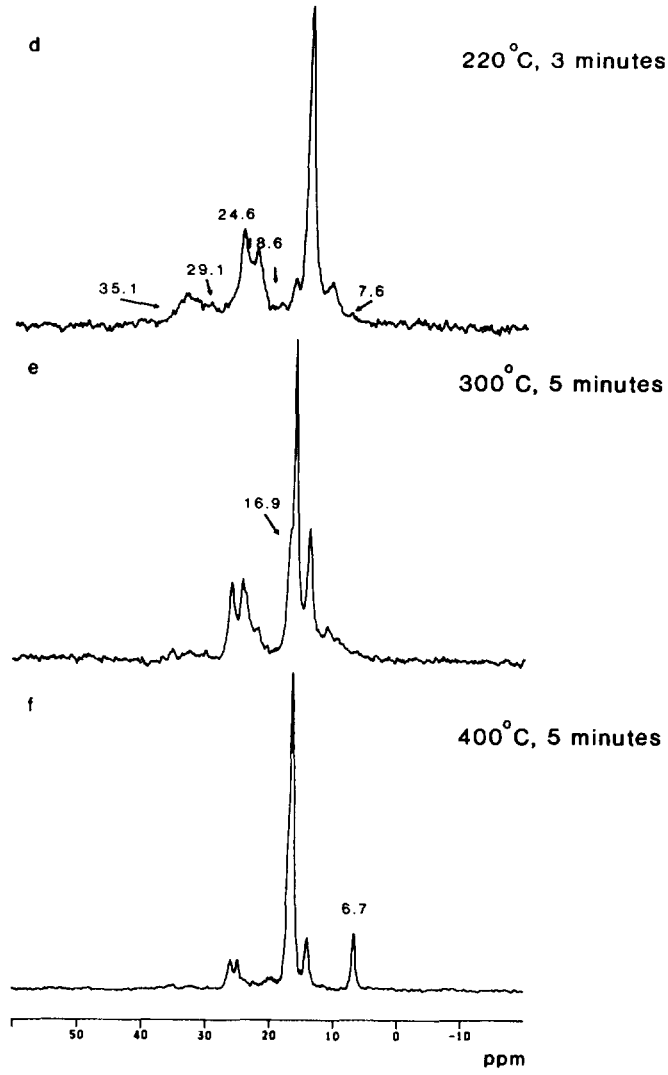

FIG. 1—*Continued*

a very small shoulder at 16.4 ppm is observed beside the main *n*-hexane-C_1 peak. This shoulder is assigned to propane, which means that cracking reactions already occur at this temperature. The conversion of *n*-hexane is indicated more clearly in Fig. 1c, recorded after exposure of the system to 200°C for 5 min. The propane signal can now be identified more definitely as a separate peak and several other minor peaks at 11.3, 22.4, and 26.0 ppm from 2- and 3-methylpentane and *n*-butane become visible. In general, up to 200°C, we observe conversion of *n*-hexane, resulting in a small but significant amount of smaller molecules and hexane isomers.

Interestingly, after exposure of the system to a slightly higher temperature of 220°C, several new species are seen (Fig. 1d). The peaks are assigned to ethane, 3-methylpentane, propane, 2-methylpentane, and *i*-butane. Clearly, more reactant has

been converted, although some residual *n*-hexane is present, as indicated by the peaks at 14.2 and 33.4 ppm. In general, this spectrum shows that a number of hexane isomers as well as primary products from cracking reactions have been formed. No evidence of the occurrence of the dimethylbutanes was observed in any of the spectra.

At 300°C, *n*-hexane peaks are no longer detected. The intense peak at 16.1 ppm in the spectrum (Fig. 1e) originates from propane. Also *i*-butane, *n*-butane, and ethane are detected. Only minor quantities of 3-methylpentane remain, whereas 2-methylpentane is virtually absent. This indicates that a higher proportion of cracking has occurred than before. In line with these findings, at 400°C a much simpler spectrum (Fig. 1f) results. The peaks can be assigned to ethane (6.7 ppm), propane (16.1 ppm), *n*-butane (13.8 and 26.0 ppm), and *i*-butane (24.6 ppm). The spectrum indicates that neither *n*-hexane nor the methylpentanes are present. Clearly, they have been cracked.

Flow Reactor/GC Experiments

For the comparison with the NMR experiments it is sufficient to include results obtained from the flow reactor/GC system at higher conversions. The variation in product distribution for conversions above 20% is given in Figs. 2a–2d for methane, ethene, ethane, propene, propane, iso-butane, *n*-butane, the butenes, pentanes, and pentenes, and the hexane isomers. In this range the relation between conversion and product yield is linear for all products. At low conversions propene and propane are the most abundant products (Fig. 2b). The initial paraffin/olefin ratio of the products is close to unity, which is in agreement with the formation of one saturated and one unsaturated molecule per cracked *n*-hexane molecule. All olefins show a decreasing yield with increasing conversion supporting the notion of prolonged contact time and an increased probability for primary products to react further. At high conversions the paraffin/olefin ratio increases, suggesting the formation of unsaturated deposits on the catalyst. Due to the small H/C ratio of such deposits and the consequently inefficient cross-polarization of the carbon nuclei via surrounding protons, such deposits cannot be observed by the CP MAS NMR technique (*16*). Significant amounts of isomers of hexane are detected at low conversions. They then decrease to very low values. It may not be deduced, however, that isomerization does not occur at higher conversions. The smaller amount of isomerization products can also be explained by the increased cracking of isomers.

DISCUSSION

The evolution of the product distributions as a function of temperature as observed in the NMR experiments is summarized in Table 3. Most noticeable in all product distribution is the absence of olefinic products. This appears to be contrary to the results from flow reactor/GC experiments shown in Fig. 2. In order to explain this the two experiments have to be compared carefully. In the NMR experiment the loading is approximately one *n*-hexane molecule per acid site. Exposure of the system to high temperature will cause cracking of some molecules into a paraffin and an olefin. The olefins, being the more reactive species, take part in secondary reactions such as oligomerization and polymerization, thus preventing an adsorption/desorption equilibrium of olefins. At this stage the catalyst has not reached steady state and is still highly active. In the flow experiments, on the other hand, the catalyst is tested under steady-state conditions, when every active site has catalyzed a large number of reactions and some deactivation may have occurred. Furthermore, due to the constant flow of reactants and products in the system the adsorption/desorption equilibrium of the olefins allows the detection of unreacted olefins. As a consequence the comparison between the two experiments is limited to high conversions in the flow reactor/GC experiments. It is possible to estimate a product distribution at

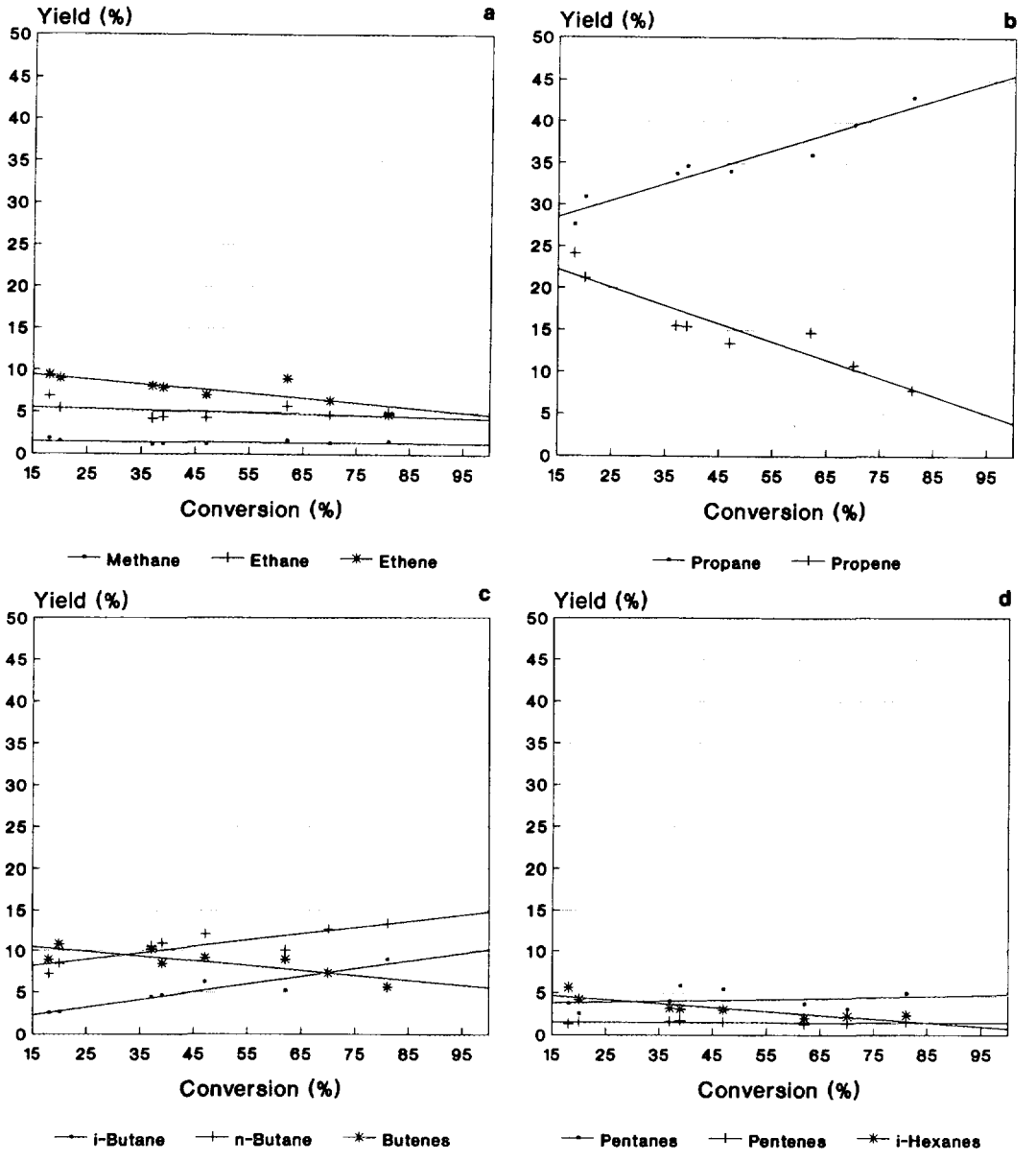

FIG. 2. Product yields from flow reactor/GC experiments in mol% as function of conversion of (a) methane, ethane, and ethene; (b) propane and propene; (c) i-butane, *n*-butane, and butenes; and (d) pantanes, pentenes, and i-hexanes.

100% conversion by extrapolation using the fitted lines in Fig. 2. Table 4 shows such an estimate for all the observed products. Assuming a detection limit of 5% (molar) in the NMR experiment it is expected that the observed product distribution consists of saturated hydrocarbons only. The butenes, pentenes, and pentanes are shown as blocks and the single components of these fractions will also lie below the detection limit. Ethane, with a predicted yield of approximately 4%, is observed by NMR.

TABLE 3

Product from the Conversion of *n*-Hexane over ZSM-5

Sample	Temperature (°C)	Observed molecules
A	20	*n*-Hexane
B	155	*n*-Hexane, propane
C	200	*n*-Hexane, propane, 3-methylpentane, 2-methylpentane, *n*-butane
D	220	*n*-Hexane, propane, 3-methylpentane, 2-methylpentane, ethane, *i*-butane, *n*-butane
E	300	Propane, *i*-butane, *n*-butane, 3-methylpentane, ethane
F	400	Propane, ethane, *i*-butane, *n*-butane

Note. The major fraction is listed first, the smallest fraction is named last.

From the product distributions observed in the NMR experiments shown in Table 3 a number of conclusions can be drawn about the reactions involved in the conversion of *n*-hexane. Assuming that both the classical carbenium ion mechanism and the protolytic mechanism can occur (*6*), and that the structure of the intermediate in the carbenium ion mechanism is best described by the carbenium ion and the corresponding alkoxide (*10, 11, 17*) as limiting structures, a reaction scheme can be set up. The basis for this scheme is the interconversion between *n*-hexane and the two methylpentanes. Evidence for the occurrence of the dimethylbutanes was not seen in the NMR experiments and only negligible amounts of 2,3-dimethylbutane were observed in the flow reactor/GC experiments. This suggests that the actual formation of the dimethylpentanes is inhibited by ZSM-5 and not only their diffusion.

TABLE 4

Estimated Product Distribution for *n*-Hexane Cracking at 100% Conversion

Product	Yield (mol%)
Methane	1.0
Ethane	4.0
Ethene	4.0
Propane	47.0
Propene	4.0
i-Butane	10.0
n-Butane	15.0
Butenes	5.0
Pentanes	5.0
Pentenes	2.0
i-Hexanes	1.0
Total	98.0

It was shown earlier that fewer dimethylbutanes are produced in the conversion of *n*-hexane by H–ZSM-5 compared to H–Y (*1*). Since those experiments were performed under flow conditions they left open the possibility that the equilibrium in the pores of the two zeolites is similar but that the dimethylbutanes can desorb only from the large-pore zeolite. Since the NMR experiment is selective for species inside the zeolite pores the conclusion can be drawn that, in contrast to H–Y (*1*), the dimethylbutanes are not formed to any appreciable extent in H–ZSM-5 and that the isomerization of *n*-hexane includes the *n*-alkane and the two methylpentanes only.

The proposed isomerization of *n*-hexane in H–ZSM-5 is shown schematically in Fig.

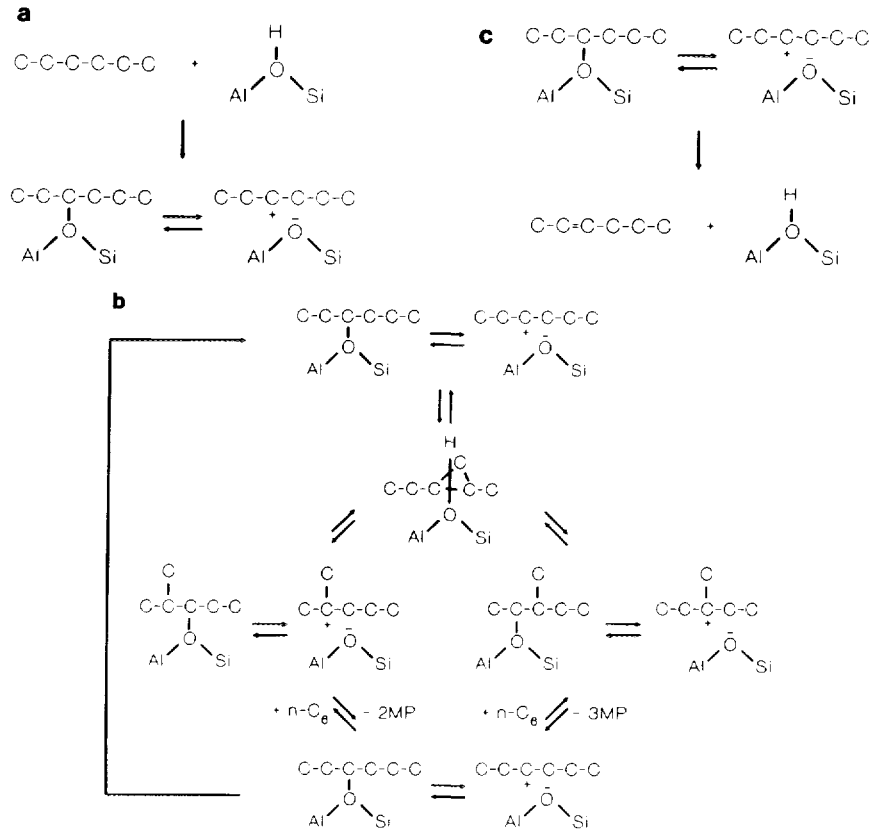

FIG. 3. The isomerization of *n*-hexane to give 2- and 3-methylpentane: (a) initiation via the loss of hydrogen to form an intermediate, (b) propagation involving isomerization and bimolecular hydride transfer, and (c) termination by the desorption of an olefin.

3. In the initiation the protonation of *n*-hexane leads to the loss of hydrogen from a carbonium ion and the formation of an intermediate (Fig. 3a). The reaction is propagated by a bimolecular hydride transfer step between an intermediate and *n*-hexane. Part of this reaction step is an isomerization of the intermediates, probably via a structure containing a cyclopropyl ring (Fig. 3b). This has been observed to occur in the interconversion of *n*-hexane into the singly branched methylpentanes using superacids (*18*) and it has also been proposed recently for hydrocarbon conversions catalysed by zeolites (*19*). The result of the bimolecular hydride transfer between the isomerized intermediates and *n*-hexane is the formation of 2- and 3-methylpentane, both of which were shown to be present in the pores of the zeolite in the NMR experiments. The newly formed *n*-hexyl intermediate then undergoes the same cycle. Termination occurs by the desorption of either *n*-hexene or one of the methylpentenes (Fig. 3c).

As exemplified by the spectrum observed at 220°C, the formation of 2- and 3-methylpentane are the major processes at that temperature. At higher temperatures the contribution of cracking increases. This can occur either from the straight-chain or branched intermediates or from the various products of the propagation step shown in Fig. 3b. The former involves a β-scission of the carbenium ions obtained from the intermediates, whereas the latter involves the α-scission of the carbonium ions formed from *n*-hexane and the two methylpentanes.

It has been shown previously that the isomerization of *n*-butane proceeds slowly compared to the isomerization of *n*-pentane (*20*). Such an isomerization is also possible when alkoxide-like species are involved, but it is expected to be even slower because, apart from steric hindrance, it would involve the breaking of the C–O bond. From the present results it is concluded that the formation of *i*-butane is a direct consequence of the skeletal isomerization of *n*-hexane. *i*-Butane is formed from either the 2-methylpentyl intermediate by β-scission or from 2-methylpentane by α-scission. This is in agreement with earlier work on the isomerization and cracking of ^{13}C-labelled branched hexanes (*21*). It was demonstrated that 2-methylpentane, 3-methylpentane, and 2,3-dimethylbutane are in equilibrium in H-mordenite and that 2-methylpentane has the highest probability of being cracked at 170°C. In another wide-pore zeolite, H–Y, 2,3-dimethylbutane was also formed (*1*). Furthermore, the cracking of 2-methylpentane over a zeolite HY yielded almost four times as much i-butane as *n*-butane (*22*). At low temperatures, it is expected that the preferred cracking route yields two product pairs from the β-scission of 2-methylpentyl species: propene/propane and ethene/*i*-butane. The driving force for the formation of *i*-butane may be the formation of the stable tertiary butyl carbenium ion. At higher temperatures monomolecular cracking becomes more important. Since this is less selective for the structure of the reactant more *n*-butane is expected as cracking product from *n*-hexane and 3-methylpentane. This is reflected in the relative amounts of *i*- and *n*-butane observed in this work. At 220°C (Fig. 1d) considerably more *i*-butane than *n*-butane is observed, whereas at 300 and 400°C comparable amounts are detected (Figs. 1e and 1f). In the flow reactor experiment more *n*-butane than *i*-butane is observed at 450°C (Fig. 2c). At even higher temperatures smaller amounts of *i*-butane are expected in the product distribution since the contribution of isomerization with respect to monomolecular cracking of *n*-hexane decreases.

CONCLUSIONS

A number of conclusions can be drawn from the comparison between *in situ* NMR experiments using closed capsules and flow reactor/GC experiments of the conversion of *n*-hexane over zeolite ZSM-5.

The results reflect two main differences in the reaction conditions. In the NMR experiment the total number of reactions catalysed by the active sites is small. The catalyst remains highly active so that olefinic cracking products are likely to react further before they are detected in the NMR experiment; no adsorption/desorption equilibrium of the olefins can form. In the flow reactor/GC experiments active sites experience deactivation to some degree and the continuous flow of reactants and products allows some olefinic products to be detected. Ideally, the two techniques would be combined in one experiment, where NMR identifies species in the reactor and the postbed analysis is performed by GC methods.

Varying the reaction temperature showed that feed isomerization is an important process in the cracking of *n*-hexane. From about 200°C cracking influences the equilibration of the different hexane isomers. The results show that 2-methylpentane is the most likely hexane isomer to be cracked at temperatures around 200°C, yielding *i*-butane. At higher temperatures the monomolecular mechanism becomes more prominent, leading to a lower selectivity in the cracking of hexane isomers. More *n*-butane is formed. A reaction scheme is proposed which has as its basic conversion the equilibrium between *n*-hexane, 2-methylpentane, and 3-methylpentane. β-Scission occurs preferentially through 2-methylpentane at temperatures around 220°C, and at higher temperatures the contribution of monomolecular cracking reactions of all three iso-

mers increases. A similar reaction scheme has been proposed earlier for the conversion of *n*-heptane (*23*), and we believe that the same is true for all longer hydrocarbon molecules, as well as for primary cracking products higher than butane and for oligomerization products obtained from secondary reactions.

ACKNOWLEDGMENT

We are grateful to Dr. A. L. Farragher for his critical comments on the manuscript of this paper.

REFERENCES

1. Guisnet, M., and Perot, G., *in* "Proceedings of the NATO Advanced Study Institute on Zeolites: Science and Technology, Alcabideche, 1983," p. 397. Martinus Nijhoff, The Hague, 1984.
2. Weitkamp, J., *in* "Proceedings of the Ketjen Catalysts Symposium 88, Scheveningen, 1988," paper G3. H. J. Lovink, Amersfoort Akzo Chemicals.
3. Dwyer, J., Dewing, J., Karim, K., Holmes, S., Ojo, A. F., Garforth, A. A., and Rawlence, J. D., *in* "Zeolite Chemistry and Catalysis" (P. A. Jacobs, N. I. Jaeger, L. Kubelková, and B. Wichterlová, Eds.), Studies in Surface Science and Catalysis, Vol. 69, p. 1. Elsevier, Amsterdam, 1991.
4. Wielers, A. F. H., Vaarkamp, M., and Post, M. F. M., *J. Catal.* **127,** 51 (1991).
5. Shigeishi, R., Garforth, A. A., Harris, I., and Dwyer, J., *J. Catal.* **130,** 423 (1991).
6. Haag, W. O., and Dessau, R. M., *in* "Proceedings, 8th International Congress on Catalysis, Berlin, 1984," Vol. 2, p. 305. Dechema, Frankfurt am Main, 1984.
7. Greensfelder, B. S., Voge, H. H., and Good, G. M., *Ind. Eng. Chem.* **41,** 2573 (1949).
8. Olah, G. A., Halpern, Y., Shen, J., and Mo-Y, K., *J. Am. Chem. Soc.* **93,** 1251 (1971); **95,** 4960 (1973).
9. Anderson, M. W., and Klinowski, J., *Nature* **339,** 200 (1989); *J. Am. Chem. Soc.* **112,** 10 (1990).
10. Datema, K. P., Nowak, A. K., Van Braam Houckgeest, J., and Wielers, A. F. H., *Catal. Lett.* **11,** 267 (1991).
11. White, J. L., Lazo, N. D., Richardson, B. R., and Haw, J. F., *J. Catal.* **125,** 260 (1990).
12. Xu, Y., Grey, C. P., Thomas, J. M., and Cheetham, A. K., *Catal. Lett.* **4,** 251 (1990).
13. Stach, H., Lohse, U., Thamm, H., and Schirmer, W., *Zeolites* **6,** 74 (1986).
14. Levy, G. C., and Nelson, G. L., "Carbon-13 NMR for Organic Chemists." Wiley–Interscience, New York, 1972.
15. Anderson, M. W., Occelli, M. L., and Klinowski, J., *J. Phys. Chem.* **96,** 388 (1992).
16. Abragam, A., "Principles of Nuclear Magnetism," International Series of Monographs on Physics. Clarendon, Oxford, 1961.
17. Kazansky, V. B., and Senchenya, I. N., *J. Catal.* **119,** 108 (1989).
18. Brouwer, D. M., and Hogeveen, H., *Prog. Phys. Org. Chem.* **9,** 179 (1972).
19. Tiong Sie, S., *Ind. Eng. Chem. Res.* **31,** 1881 (1992).
20. Daage, M., and Fajula, F., *J. Catal.* **81,** 394 (1983).
21. Beecher, R., and Voorhies, A., Jr., *Ind. Eng. Chem. Prod. Res. Dev.* **8,** 3607 (1969).
22. Abbot, J., and Wojciechowski, B. W., *J. Catal.* **113,** 353 (1988).
23. Corma, A., Planelles, J., and Tomás, F., *J. Catal.* **94,** 445 (1985).